Science
AAAS

Lethal Interactions Between Parasites and Prey Increase Niche Diversity in a Tropical Community

Marty A. Condon *et al.*

Science **343**, 1240 (2014);
DOI: 10.1126/science.1245007

This copy is for your personal, non-commercial use only.

If you wish to distribute this article to others, you can order high-quality copies for your colleagues, clients, or customers by clicking here.

Permission to republish or repurpose articles or portions of articles can be obtained by following the guidelines here.

The following resources related to this article are available online at www.sciencemag.org (this information is current as of April 13, 2014):

Updated information and services, including high-resolution figures, can be found in the online version of this article at:
http://www.sciencemag.org/content/343/6176/1240.full.html

Supporting Online Material can be found at:
http://www.sciencemag.org/content/suppl/2014/03/12/343.6176.1240.DC1.html

A list of selected additional articles on the Science Web sites **related to this article** can be found at:
http://www.sciencemag.org/content/343/6176/1240.full.html#related

This article **cites 37 articles**, 9 of which can be accessed free:
http://www.sciencemag.org/content/343/6176/1240.full.html#ref-list-1

This article has been **cited by** 1 articles hosted by HighWire Press; see:
http://www.sciencemag.org/content/343/6176/1240.full.html#related-urls

This article appears in the following **subject collections:**
Ecology
http://www.sciencemag.org/cgi/collection/ecology

Downloaded from www.sciencemag.org on April 13, 2014

Science (print ISSN 0036-8075; online ISSN 1095-9203) is published weekly, except the last week in December, by the American Association for the Advancement of Science, 1200 New York Avenue NW, Washington, DC 20005. Copyright 2014 by the American Association for the Advancement of Science; all rights reserved. The title *Science* is a registered trademark of AAAS.

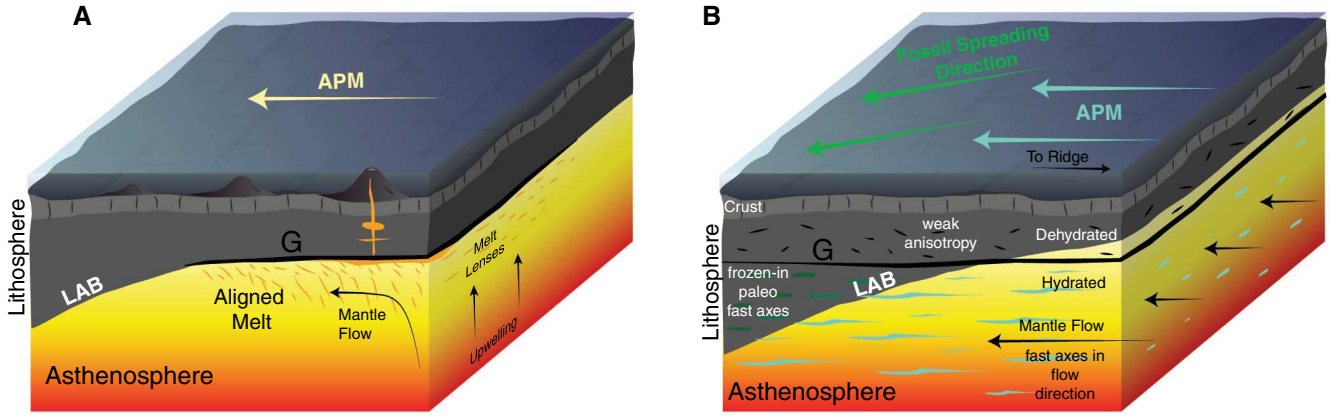

Fig. 3. Proposed models for azimuthal anisotropy beneath the Pacific and detection of the G. (**A**) The G as the top of an anisotropic entrainment and segregation of melt within the asthenosphere. Dynamical upwelling produces melt that is entrained into mantle flow and compacts at the base of the lithosphere from a solidus-induced change in permeability (*10*). The G coincides with the top of the melting zone. In the scenario where the APM and fossil spreading directions are parallel, the G would not be detected. (**B**) The G as a chemical boundary between a weakly anisotropic dry layer and a hydrated region characterized by the fossil frozen-in alignment of olivine. Olivine aligns with the present-day APM in the hydrated, warm asthenosphere. In this scenario, G can be both coincident with and above the thermally defined LAB and is detected by the *SS* precursors where the anisotropy contrast between the two layers is large.

References and Notes

1. B. Gutenberg, *Bull. Seismol. Soc. Am.* **38**, 121 (1948).
2. B. Bagley, J. Revenaugh, *J. Geophys. Res. Solid Earth* **113**, B12301 (2008).
3. H. Kawakatsu *et al.*, *Science* **324**, 499–502 (2009).
4. C. A. Rychert, P. M. Shearer, *J. Geophys. Res. Solid Earth* **116**, B07307 (2011).
5. N. Schmerr, *Science* **335**, 1480–1483 (2012).
6. Y. Tan, D. V. Helmberger, *J. Geophys. Res. Solid Earth* **112**, B08301 (2007).
7. J. B. Gaherty, M. Kato, T. H. Jordan, *Phys. Earth Planet. Inter.* **110**, 21–41 (1999).
8. G. Hirth, D. L. Kohlstedt, *Earth Planet. Sci. Lett.* **144**, 93–108 (1996).
9. S. Karato, *Earth Planet. Sci. Lett.* **321-322**, 95–103 (2012).
10. T. Sakamaki *et al.*, *Nat. Geosci.* **6**, 1041–1044 (2013).
11. Materials and methods are available on *Science* Online.
12. K. Visser, J. Trampert, B. L. N. Kennett, *Geophys. J. Int.* **172**, 1016–1032 (2008).
13. E. Debayle, Y. Ricard, *Earth Planet. Sci. Lett.* **376**, 165–177 (2013).
14. H. Yuan, B. Romanowicz, *Nature* **466**, 1063–1068 (2010).
15. A. E. Gripp, R. G. Gordon, *Geophys. J. Int.* **150**, 321–361 (2002).
16. A. M. Dziewonski, D. L. Anderson, *Phys. Earth Planet. Inter.* **25**, 297–356 (1981).
17. A. Maggi, E. Debayle, K. Priestley, G. Barruol, *Geophys. J. Int.* **166**, 1384–1397 (2006).
18. M. Nettles, A. M. Dziewonski, *J. Geophys. Res. Solid Earth* **113**, B02303 (2008).
19. C. E. Nishimura, D. W. Forsyth, *Geophys. J.* **96**, 203–229 (1989).
20. S. Karato, in *High-Pressure Research in Mineral Physics*, M. H. Manghnani, Y. Syono, Eds. (TERRAPUB/AGU, Tokyo/Washington, 1987), pp. 455–471.
21. T. Miyazaki, K. Sueyoshi, T. Hiraga, *Nature* **502**, 321–326 (2013).
22. B. H. Hager, M. A. Richards, *Philos. Trans. R. Soc. Lond. A* **328**, 309–327 (1989).
23. C. Gaboret, A. M. Forte, J. P. Montagner, *Earth Planet. Sci. Lett.* **208**, 219–233 (2003).
24. C. A. Rychert, N. Schmerr, N. Harmon, *Geochem. Geophys. Geosyst.* **13**, Q0AK10 (2012).
25. S. Naif, K. Key, S. Constable, R. L. Evans, *Nature* **495**, 356–359 (2013).
26. B. K. Holtzman, J. M. Kendall, *Geochem. Geophys. Geosyst.* **11**, Q0AB06 (2010).
27. K. J. Matthews, R. D. Muller, P. Wessel, J. M. Whittaker, *J. Geophys. Res. Solid Earth* **116**, B12109 (2011).
28. R. L. Parker, D. W. Oldenburg, *Nature* **242**, 137–139 (1973).
29. C. A. Stein, S. Stein, *Nature* **359**, 123–129 (1992).

Acknowledgments: C.B. and K.Y. were funded by NSF EAR grants 0838605 and 0949255; N.S. was funded by NSF EAR 1247608. We thank J. Trampert and K. Visser for making their phase velocity maps freely available. Partial derivatives were calculated using fortran code MINEOS (www.geodynamics.org/cig/software/mineos), and figures were made with the Generic Mapping Tools, Gnuplot, and Xmgrace. We thank P. Davis for fruitful discussions. The data used were the phase velocity maps published in (*12*) and are available at www.geo.uu.nl/~jeannot/My_web_pages/Downloads.html. The models are available in the supplementary materials.

Supplementary Materials

www.sciencemag.org/content/343/6176/1237/suppl/DC1
Materials and Methods
Supplementary Text
Figs. S1 to S27
Table S1
References (*30*–*56*)
Model file S1

2 October 2013; accepted 17 February 2014
Published online 27 February 2014;
10.1126/science.1246724

Lethal Interactions Between Parasites and Prey Increase Niche Diversity in a Tropical Community

Marty A. Condon,[1]* Sonja J. Scheffer,[2] Matthew L. Lewis,[2] Robert Wharton,[3] Dean C. Adams,[4,5] Andrew A. Forbes[6]

Ecological specialization should minimize niche overlap, yet herbivorous neotropical flies (*Blepharoneura*) and their lethal parasitic wasps (parasitoids) exhibit both extreme specialization and apparent niche overlap in host plants. From just two plant species at one site in Peru, we collected 3636 flowers yielding 1478 fly pupae representing 14 *Blepharoneura* fly species, 18 parasitoid species (14 *Bellopius* species), and parasitoid-host associations, all discovered through analysis of molecular data. Multiple sympatric species specialize on the same sex flowers of the same fly host-plant species—which suggests extreme niche overlap; however, niche partitioning was exposed by interactions between wasps and flies. Most *Bellopius* species emerged as adults from only one fly species, yet evidence from pupae (preadult emergence samples) show that most *Bellopius* also attacked additional fly species but never emerged as adults from those flies.

Plant and insect diversity both peak in the tropics (*1*) where insect diversity is strongly associated with plant diversity (*2*, *3*) and extreme specialization (*4*). Ecological specialization is often considered a driver of diversification, with increasing specialization reducing niche overlap and promoting speciation (*5*, *6*). Diversification of herbivorous insects, arguably the most diverse group of organisms on Earth (*7*), is often explained by "arms race" or "escape and radiate" hypotheses involving specialized interactions either between two trophic levels—host plants and

specialized herbivores (*8*), or among three trophic levels—plants, herbivores, and their specialized enemies (*9*–*11*). Tritrophic studies emphasize shifts to new host plants as a mechanism that can cause cascading patterns of diversification. Specifically, shifts to new "enemy-free" host plants allow herbivores to escape enemies like parasitoids (lethal parasitic wasps) that often use plant-related cues to find insect hosts (*11*); in turn, selection favors parasitoids that can respond to new plant-related cues to track their prey (*10*, *11*). These models emphasize the lethality of parasitoids; however, parasitoids can also be killed by their hosts (*12*–*14*). We suggest that such "inhospitable" (lethal) hosts may help explain high levels of diversity in some communities.

Specificity to host plants is thought to be a predictor of herbivorous insect diversity (*2*, *4*); however, diversity of some highly specialized herbivorous insect groups far exceeds predictions based purely on host plants' taxonomic diversity and architectural complexity. For example, all species in the species-rich neotropical tephritid genus *Blepharoneura* feed on plants in the family Cucurbitaceae (cucurbits). Unlike most plants, all cucurbits have unisexual flowers, and many cucurbit species are sexually dimorphic: plants bearing female flowers differ architecturally from plants bearing male flowers. Cucurbit flowers are hosts to many species of *Blepharoneura* that feed specifically on particular sex flowers of single species of plants (*15*). To our surprise, we find multiple sympatric cryptic *Blepharoneura* species feeding specifically on exactly the same tissues—the succulent fused sepals (calyces)—of the same sex flowers of the same plant species. This pattern suggests extreme niche overlap among specialists—at least in the "plant-defined dimensions" of their niches (*15*); however, niches can be defined by multiple dimensions representing all environmental factors that affect fitness of individuals (*16*)—including predators and parasites. Species sharing exactly the same food resources may not share the same enemies.

Parasitoids represent an important third trophic level in *Blepharoneura* communities, as in most other communities of herbivorous insects (*9*–*11*, *17*). Parasitoids lay their eggs inside immature *Blepharoneura* (eggs or larvae) hidden within flower tissues. The parasitized fly is not killed immediately but continues to feed on plant host material until larval development is complete and the fly forms a puparium by hardening its larval exoskeleton. The immature parasitoid feeds on the immature fly and completes metamorphosis within the fly puparium. When the wasp reaches adulthood, it emerges from the puparium, leaving behind material ("postemergence puparium") containing both the wasp and host-fly DNA.

To reveal patterns of fly and parasitoid diversity, niche overlap, and tritrophic interactions, we collected 3636 flowers representing four host-plant niches: male flowers and female flowers of two species of cucurbit vines (*Gurania acuminata* and *G. spinulosa*) growing along or near the perimeter of a 1-km-long airstrip at Los Amigos Biological Station in Madre de Dios, Peru, in October 2008 (*18*). Fewer than half of the flowers were infested by flies (Fig. 1). From those flowers, we obtained 1478 fly puparia. We used a traditional approach to individually rear 1085 puparia (*18*): we waited

[1]Department of Biology, Cornell College, Mount Vernon, IA 52314, USA. [2]Systematic Entomology Laboratory, Agricultural Research Service–U.S. Department of Agriculture (ARS-USDA), Beltsville, MD 20705, USA. [3]Department of Entomology, Texas A&M University, College Station, TX 77843, USA. [4]Department of Ecology, Evolution, and Organismal Biology, Iowa State University, Ames, IA 50011, USA. [5]Department of Statistics, Iowa State University, Ames, IA 50011, USA. [6]Department of Biology, University of Iowa, Iowa City, IA 52242, USA.

*Corresponding author. E-mail: mcondon@cornellcollege.edu

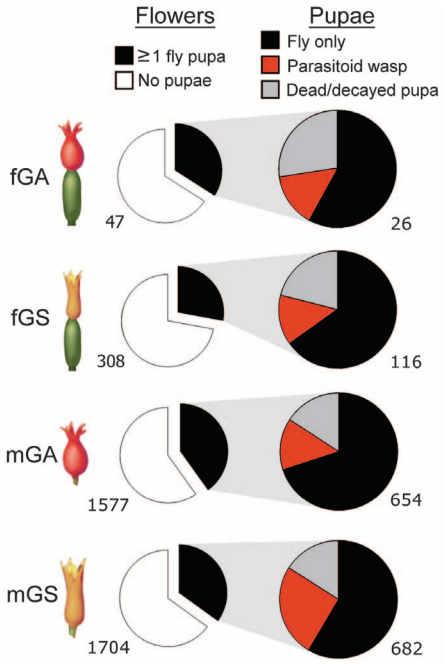

Fig. 1. Percentage of *Gurania* flowers infested by immature *Blepharoneura* flies (left) and survivorship of flies (right) revealing many uninfested flowers and parasitoid-free flies. Fly only: adult flies and preemergence puparia without wasps. Parasitoid wasp: adult wasps and preemergence puparia containing wasps. Dead/decayed puparia: unknown cause of death. Flowers: f, female; m, male, GA, *Gurania acuminata*, GS, *G. spinulosa*.

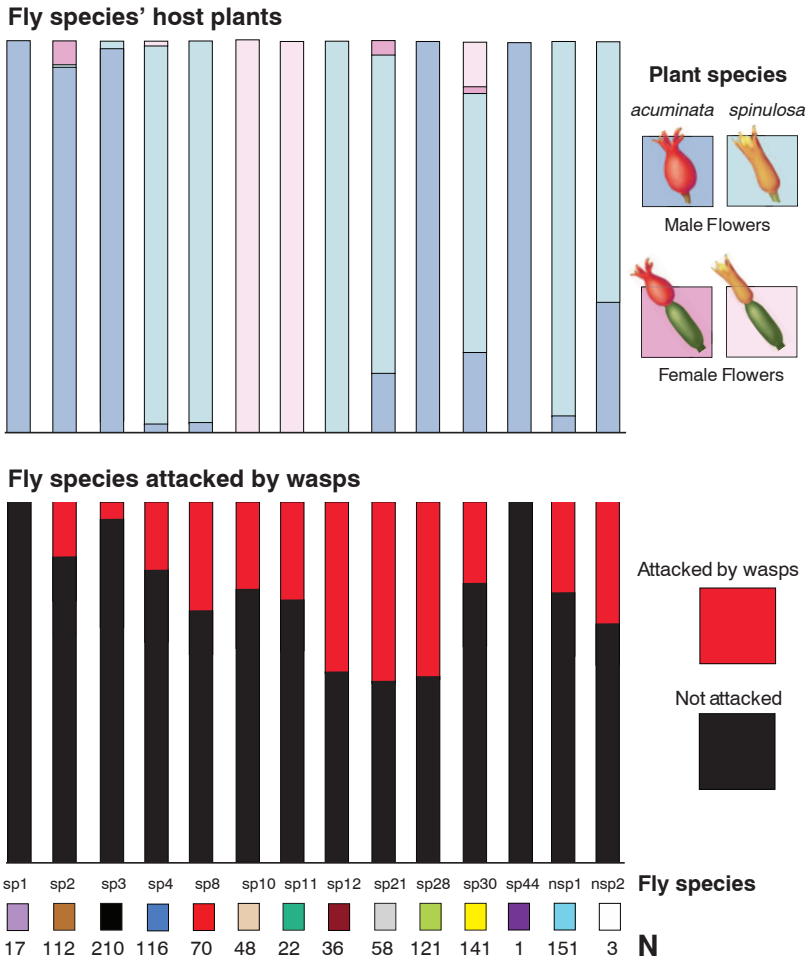

Fig. 2. *Gurania* host plants (top) used by each of 14 fly (*Blepharoneura*) species and percentage of each fly species attacked by wasps (bottom). Samples (*N*) include pre- and postemergence flies. Fly species were color-coded as in Figs. 3 and 4, and figs. S1 to S8.

for adults (either a single fly or a single wasp) to emerge from each puparium. We preserved those adults and associated postemergence puparia in ethanol. Instead of rearing the remaining 393 puparia to adulthood, we used ethanol to kill and preserve newly formed puparia ("preemergence") shortly after pupariation, before adult fly or wasp emergence.

To identify fly species, we used mitochondrial cytochrome oxidase I (mtCOI) sequences (*18*) previously corroborated by nuclear data (*15*). To identify parasitoid species, we sorted wasps into morphospecies, analyzed sequences of mtCOI and nuclear genes 28S and ef1-α, and genotyped a panel of 155 amplified fragment length polymorphism (AFLP) loci (*18*). To determine the host (fly) species killed by each wasp, we extracted DNA from the postemergence puparium of each adult wasp and used fly-specific primers to preferentially amplify fly mitochondrial DNA (mtDNA) (*18*). Postemergence wasp-fly associations represent successful (lethal to flies) host use by wasps. We also used preemergence puparia to assess wasp-fly associations. We extracted preemergence puparial DNA and used taxon-specific mtCOI primers to independently amplify fly mtCOI (always present) and wasp mtCOI (if present). Preemergence wasp-fly data include associations that would have been successful (lethal to flies) as well as "inhospitable" associations that would not have been successful (lethal to wasps). Comparison of post-and preemergence wasp-fly associations can expose virulence at two trophic levels: wasps lethal to flies, and flies inhospitable (lethal) to wasps.

We found extraordinary diversity. In just these two plant species at this single site in Peru, we found 14 fly species (all *Blepharoneura*) and 18 parasitoid species (*18*) (figs. S1 to S7). Most parasitoids were braconid wasps in the subfamily Opiinae (17 species): 14 *Bellopius* species (n = 199 individuals), two *Thiemanastrepha* species (n = 50), and one *Utetes* species (n = 2). We also reared a figitid wasp species (n = 62) (*18*). The level of parasitism of each fly species ranged from zero (*Blepharoneura* sp1) (Fig. 2) to ~50% (sp21 and sp28) (Fig. 2). Although wasp abundance was correlated with host-fly abundance (r = 0.58) (fig. S8a), the relative proportion of each fly species that was parasitized was independent of fly abundance (r = –0.05) (fig. S8b).

Multiple species occupied each of the four host-plant resources (two flower sexes of each of two host-plant species). For example, nine fly species and 12 parasitoid species were discovered in male flowers of *G. spinulosa* (Figs. 2 and 3). Most fly species in this system are extreme specialists: 11 of 14 fly species feed primarily (≥ 90% of individuals) on a single tissue of a single host-plant species (Fig. 2 and fig. S1). Most parasitoid species are even more specific to the host plants of their fly hosts: All but 1 of the 11 species of *Bellopius* represented by more than one specimen exhibited complete (100%) fidelity to a single plant-host species and to a single flower sex (Fig. 3).

Bellopius wasps also discriminate among fly species sharing identical plant resources. As many as 11 *Blepharoneura* fly species infest a single plant resource (Fig. 2) and would be available to parasitoids visiting that plant resource, yet adult *Bellopius* parasitoids revealed a pattern of extreme specialization. Ten of the 11 species of *Bellopius* represented by more than one adult emerged from its "own" single species of *Blepharoneura* (Fig. 3), which revealed a high level of niche partitioning (not niche overlap) among wasps that successfully kill flies. Similarly, mortality suffered by each fly species was usually caused by a single species of *Bellopius*. Of the 10 fly species killed by *Bellopius*, 7 were killed by a single species (Figs. 3 and 4). Such diversity and specificity is especially remarkable because the two vine species grew very close together—often intertwined. Single individual plants served as hosts to as many as six species of flies (table S9), yet all but one species of *Bellopius* (a member of poorly defined *Bellopius* group E1c) (fig. S7 and table S10) visiting those plants successfully parasitized only one species of fly. Such extreme specialization reveals a clear pattern of niche partitioning among the parasitoids, which in turn adds unique dimensions (defined by specific parasitoids) to each fly species' niche (Fig. 4).

A different pattern, however, emerges from analysis of preemergence puparia (Fig. 3). Of the 11 species of *Bellopius* detected within more than one preemergence fly puparium, 8 species were found in puparia of more than one species of *Blepharoneura*. The difference between the pre- and postemergence samples is biologically informative (table S8) (Fisher's exact test, P = 0.0075; confirmed by permutation test, P = 0.0001) (fig. S10): Preemergence puparia show that eight species of *Bellopius* oviposited into more than one species of fly, but reared samples show that adults of each species of *Bellopius* (all but species L) emerged from just a single species of *Blepharoneura*.

Comparison of pre- and postemergence samples suggests that each fly species can defend itself (perhaps immunologically) against most species of *Bellopius*. Offspring of wasps that oviposit into the "wrong" fly are dead offspring (our records show no adults emerging from those fly species) (Fig. 3); thus, selection favors extremely specialized

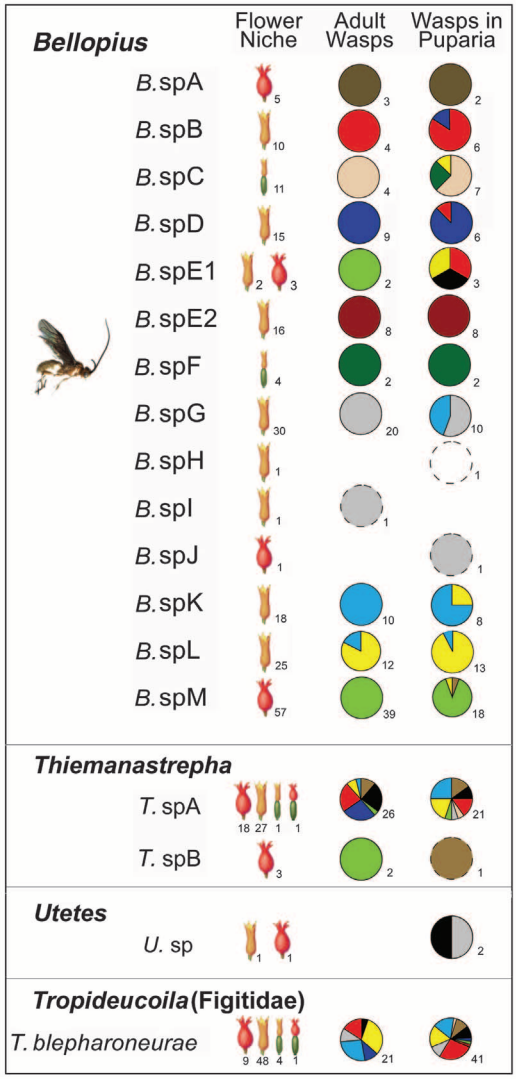

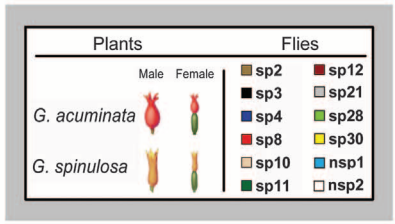

Fig. 3. Parasitoid (wasp) and host-fly associations revealed by adult wasps and preemergence puparia. Colors in pie charts represent fly species. Flower icons represent plant hosts of flies.

host choice by the wasps. Comparison of pre- and postemergence samples also reveals that wasps only oviposit into the "wrong" fly species when their primary host is found on the same flowering branch (table S9) (Fisher's exact test, $P = 0.0155$), which implies that wasps can identify that their host fly is present on a plant but can less accurately discriminate among individual larvae feeding within flowers.

The *Bellopius* pattern contrasts sharply with patterns of specificity shown by other parasitoids reared from *Blepharoneura*. For example, the two species of *Thiemanastrepha* reared from these *Blepharoneura* are generalists and attack 10 species of flies in all four plant-defined niches (Fig. 3); at least seven species of *Blepharoneura* are vulnerable to the most abundant species of *Thiemanastrepha* (Fig. 3). The single figitid species (*Tropideucoila blepharoneurae*) found in this study also attacked 10 different fly species (Fig. 3).

Insects have a well-developed immune system, and the defenses of larval flies against their internal parasitoids are particularly well-studied (*12*–*14*). *Blepharoneura* flies' defenses against *Bellopius* parasitoids represent a "hidden" niche dimension revealed through analysis of preemergence puparia (Figs. 3 and 4). In this tropical system, specialized parasitoids' offspring die in the "wrong" species of fly. Thus, selection favors parasitoids able to discriminate among multiple sympatric species of flies infesting the same host plants. Fidelity to host-plant parts and host-plant species increases *Bellopius* parasitoids' chances of detecting the "correct" host-fly species, but such fidelity also provides opportunities for flies to escape (Fig. 4): Flies on alternate host-plant parts (or alternate host-plant species) escape detection by their specialized lethal parasitoid(s), which oviposit primarily into a particular part and species of plant (Figs. 3 and 4). Yet, in this system, "escape" is not the only defense against parasitoids: Inhospitable flies are lethal to parasitoids.

Instead of representing an example of extreme niche overlap (*15*), this highly diverse community of 14 fly species and 14 *Bellopius* parasitoid species, all occupying flowers of just two species of plants, represents a community with nonoverlapping niches—each distinguished by lethal interactions between parasitoids and vulnerable flies and between parasitoids and inhospitable (lethal) flies (Figs. 3 and 4). Highly specific virulence (lethality) in both parasitoids and their prey adds a previously hidden but highly dynamic dimension to analyses of tritrophic interactions, which typically focus on unidirectional cascading patterns of escape via shifts in host plant use (*10*, *11*, *17*). Discovery of such insect parasitoid-prey interactions in complex communities of cryptic species depends on molecular methods to expose morphologically cryptic species and reveal interactions (*15*, *19*, *20*). Future studies using molecular genetic methods to identify species in other communities throughout the Neotropics are likely to reveal a geographic mosaic (*21*) of highly diverse and dynamic interactions driven by "escape and radiate" mechanisms not only at the level of host plant use, but also at the level of virulent interactions.

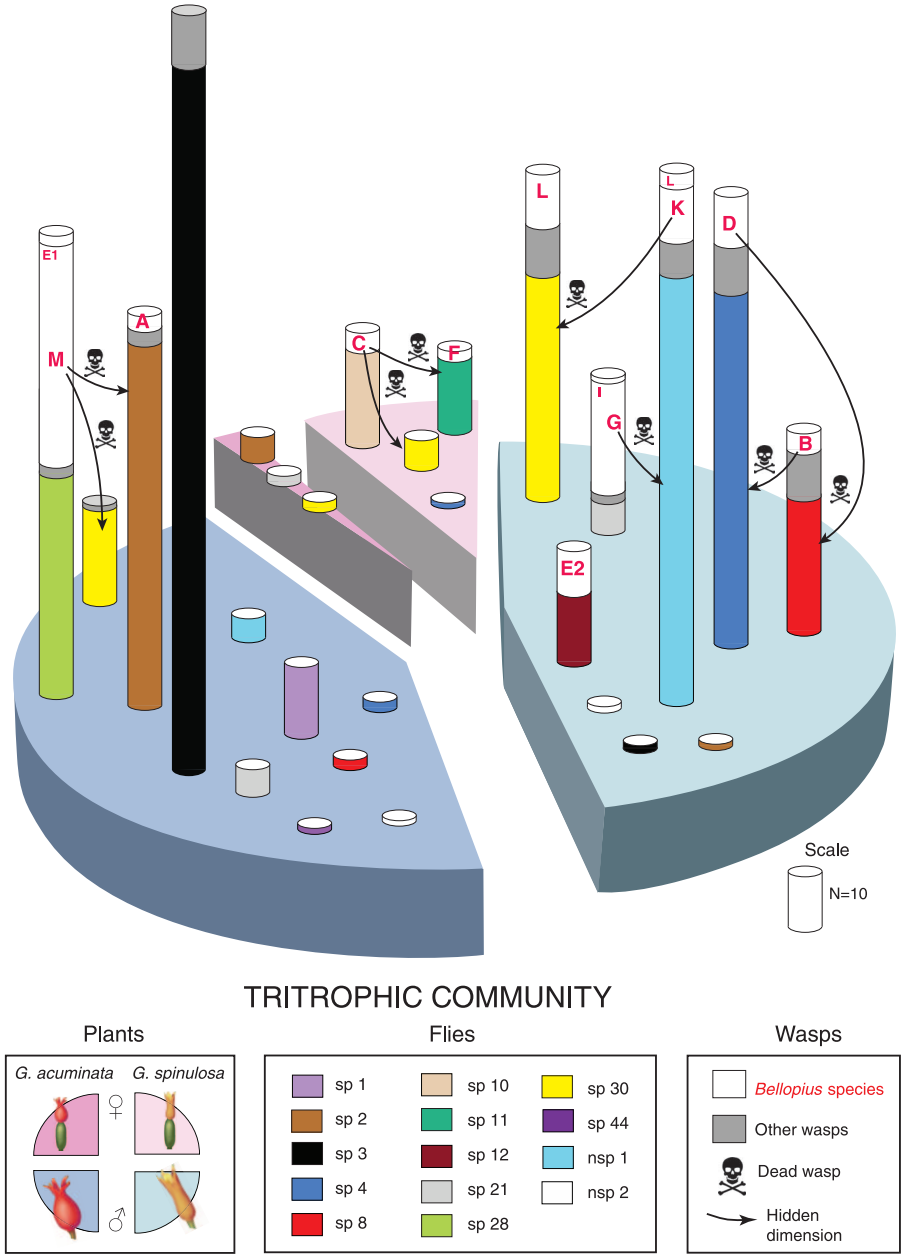

Fig. 4. Tritrophic community and "hidden" lethal interactions: plant hosts (basal pie chart, *N* = 729 host flowers) yielding adult flies and parasitoids. Stacked bars (columns) represent numbers of reared adults: bottom of bars, flies designated by colors; middle, generalist parasitoids (dark gray); and top of bar (white), lethal *Bellopius* species (red letters). (Small letters indicate rare *Bellopius*.) Arrows from *Bellopius* parasitoids indicate host flies from which adult wasps never emerged.

References and Notes

1. E. O. Wilson, *The Diversity of Life* (Norton, New York, 1999).
2. V. Novotny *et al.*, *Science* **313**, 1115–1118 (2006).
3. Y. Basset *et al.*, *Science* **338**, 1481–1484 (2012).
4. L. A. Dyer *et al.*, *Nature* **448**, 696–699 (2007).
5. C. Darwin, *On the Origin of Species by Means of Natural Selection or the Preservation of Favored Races in the Struggle for Life* (J. Murray, London, 1859).
6. D. Schluter, *The Ecology of Adaptive Radiation* (Oxford Univ. Press, Oxford, 2000).
7. D. R. Strong, J. H. Lawton, R. Southwood, *Insects on Plants: Community Patterns and Mechanisms* (Harvard Univ. Press, Cambridge, MA, 1984).
8. P. R. Ehrlich, P. H. Raven, *Evolution* **18**, 586–608 (1964).
9. P. R. Price *et al.*, *Annu. Rev. Ecol. Syst.* **11**, 41–65 (1980).
10. J. O. Stireman III, J. D. Nason, S. B. Heard, J. M. Seehawer, *Proc. Biol. Sci.* **273**, 523–530 (2006).
11. A. A. Forbes, T. H. Q. Powell, L. L. Stelinski, J. J. Smith, J. L. Feder, *Science* **323**, 776–779 (2009).
12. B. Lemaitre, J. Hoffmann, *Annu. Rev. Immunol.* **25**, 697–743 (2007).
13. A. R. Kraaijeveld, H. C. J. Godfray, *Am. Nat.* **153** (s5), S61–S74 (1999).

14. S. A. Mohamed, W. A. Overholt, R. A. Wharton, S. A. Lux, E. M. Eltoum, *Biol. Control* **28**, 155–163 (2003).
15. M. A. Condon, S. J. Scheffer, M. L. Lewis, S. M. Swensen, *Science* **320**, 928–931 (2008).
16. J. M. Chase, M. A. Leibold, *Ecological Niches: Linking Classical and Contemporary Approaches* (Univ. of Chicago Press, Chicago, 2003).
17. M. S. Singer, J. O. Stireman III, *Ecol. Lett.* **8**, 1247–1255 (2005).
18. Materials and methods are available as supplementary materials on *Science* Online.
19. M. A. Smith *et al.*, *Proc. Natl. Acad. Sci. U.S.A.* **105**, 12359–12364 (2008).
20. A. Veijalainen *et al.*, *Proc. Biol. Sci.* **279**, 4694–4698 (2012).
21. J. N. Thompson, *The Geographic Mosaic of Coevolution* (Univ. of Chicago Press, Chicago, 2005).

Acknowledgments: Funding: NSF-0330845, 0949361 to M.A.C.; NSF 0949027 to R.W.; NSF ROA (1145355), University of Iowa to A.A.F. Data are available in supplementary materials and archived at National Center for Biotechnology Information, NIH, GenBank (accession numbers: KF473465 to KF475237). The Instituto Nacional de Recursos Naturales-Intendencia Forestal y de Fauna Silvestre del Perú authorized collections (autorización no. 110-2008-INRENA-IFFS-DCB) and exportation of specimens (permiso no. 011832-AG-INRENA). T. Litwak assisted with illustrations. The authors declare no conflicts of interest. USDA is an equal opportunity provider and employer.

Supplementary Materials
www.sciencemag.org/content/343/6176/1240/suppl/DC1
Materials and Methods
Figs. S1 to S9
Tables S1 to S10
References (*22*–*49*)

21 August 2013; accepted 29 January 2014
10.1126/science.1245007

Structure of Human RNase L Reveals the Basis for Regulated RNA Decay in the IFN Response

Yuchen Han,* Jesse Donovan,* Sneha Rath,* Gena Whitney, Alisha Chitrakar, Alexei Korennykh†

One of the hallmark mechanisms activated by type I interferons (IFNs) in human tissues involves cleavage of intracellular RNA by the kinase homology endoribonuclease RNase L. We report 2.8 and 2.1 angstrom crystal structures of human RNase L in complexes with synthetic and natural ligands and a fragment of an RNA substrate. RNase L forms a crossed homodimer stabilized by ankyrin (ANK) and kinase homology (KH) domains, which positions two kinase extension nuclease (KEN) domains for asymmetric RNA recognition. One KEN protomer recognizes an identity nucleotide (U), whereas the other protomer cleaves RNA between nucleotides +1 and +2. The coordinated action of the ANK, KH, and KEN domains thereby provides regulated, sequence-specific cleavage of viral and host RNA targets by RNase L.

Cells of higher vertebrates respond to pathogens and damage by releasing interferons (IFNs), which activate protective programs in surrounding cells. One of the ubiquitous protective programs in mammalian tissues involves cleavage of intracellular RNA by a protein kinase family receptor, RNase L (*1*). RNase L is a latent endoribonuclease encoded by the hereditary prostate cancer 1 (HPC1) locus and activated by the second messenger, 2-5A (2′,5′-linked oligoadenylates of variable length) (*1*). In human cells, 2-5As are synthesized by IFN-induced 2-5A synthetases, which serve as sensors of pathogen- and damage-associated double-stranded RNA (dsRNA) (*2*, *3*). The activation of RNase L thus depends on the action of IFNs and accumulation of dsRNA.

Here, we report two crystal structures of human RNase L (table S1). These structures and complementary functional studies reveal the mechanism of 2-5A sensing and RNA cleavage by RNase L and suggest that a similar mechanism of RNA cleavage operates during regulated Ire1-dependent decay (RIDD) (*4*). We obtained diffracting crystals of nearly full-length human RNase L using cocrystallization with 2-5A, nucleotides, and an RNA 18-nucleotide oligomer 5′-GGCUUUUGACCUUUAUGC-3′ (RNA18). Cocrystallization with RNA18 was enabled by the use of a catalytically inactive RNase L mutant H672N. The final construct includes residues 21 to 719. A version of this construct with a wild-type (WT) active site is catalytically active in solution.

We determined structures of two RNase L complexes, which crystallized in different space groups (table S1). Both complexes reveal the same crossed homodimer that buries >8000 $Å^2$ of surface area (Fig. 1A). Previous solution studies indicated that RNase L can form dimers and higher-order oligomers (*5*). Modeling based on the oligomer of Ire1 (*6*) predicts that the homodimers of RNase L could form a similar assembly. The kinase homology (KH) domain of RNase L has a typical protein kinase fold with two globular lobes (Fig. 1B). Adenosine diphosphate (ADP) and β,γ-methyleneadenosine triphosphate are bound to the KH domain in the same conformation as ADP in the catalytically active protein kinase Ire1 (fig. S1, A to C). Nonhydrolyzable nucleotides and ATP exhibit the same effect on RNase L (fig. S1D), indicating that ATP hydrolysis is not involved in RNase L regulation, as suggested previously (*7*).

The KH domain lacks the conserved DFG motif found in most protein kinases and contains the DFD sequence, resembling protein kinases Mnk1/2 (*8*). RNase L does not carry out autophosphorylation (*7*), but it remains unknown whether RNase L phosphorylates nonself targets. To examine this possibility, we assayed phosphorylation of a nonspecific substrate, myelin basic protein (MBP), using Ire1 as a control kinase. Ire1 phosphorylated MBP, whereas RNase L was inactive (fig. S1E), supporting the current consensus that RNase L is a pseudokinase. The activation loop of RNase L contains only 13 amino acid residues and is among the shortest in the human protein kinome (fig. S3). The interlobe hinge and the ATP pocket contact a unique helix from the ankyrin (ANK)/KH linker (Fig. 1B and fig. S2). These attributes of the KH domain likely reflect adaptation to autophosphorylation-independent control as a homodimerization scaffold.

Previous structural studies identified two different 2-5A binding sites in the ANK domain (*5*, *9*). The crystal structure of the entire RNase L now reveals an unanticipated third site in the N lobe of the KH domain (Fig. 1A and fig. S4, A to C). The ANK and KH domains create a composite pocket for 2-5A binding, which exposes the 2′-end to solvent to accommodate long 2-5A molecules and anchors the 5′-end in the ANK domain (fig. S5A). Although RNase L can recognize 5′-p and 5′-ppp groups, at saturating concentrations 2-5pA_3 activates RNase L stronger than 2-5pppA_3 (fig. S5, B and C). The ANK/ANK homodimer binds 2-5A in a configuration that displays the phosphate p1 for recognition by the KH domain (fig. S6). Mutagenesis of the KH/2-5A interface confirms that the N lobe is functionally involved in 2-5A sensing (fig. S4D). The ANK domain contains a characteristic helix αI, which docks to the KH domain in trans upon homodimerization (fig. S7). The αI/N-lobe interaction and an ANK/N-lobe contact mediated by the residue R238 also facilitate RNase L activation by 2-5A (fig. S4, C and D).

The KH/KH and kinase extension nuclease (KEN)/KEN interfaces resemble those in Ire1 (*10*). Mutagenesis confirmed that both interfaces are important for 2-5A–dependent RNase L activation (Fig. 2A) and dimerization (fig. S8). The KEN residues involved in catalysis in Ire1 (*10*, *11*) are structurally invariant in RNase L (Fig. 2B), indicating that these enzymes share the same catalytic mechanism. However, the KEN domains contain different α-helix/loop elements (HLE) (*6*), implicated in RNA specificity (*10*). To examine the HLE function, we shortened this element in RNase L (ΔHLE). The ΔHLE mutant still cleaved RNA but exhibited a decreased rate and a greater preference for single-stranded RNA (ssRNA)

Department of Molecular Biology, Princeton University, 216 Schultz Laboratory, Princeton, NJ 08540, USA.

*These authors contributed equally to this work.
†Corresponding author. E-mail: akorenny@princeton.edu